All-optical packet switching and label rewriting for data packets beyond 160 Gb/s

Please check the document version of this publication:

• A submitted manuscript is the version of the article upon submission and before peer-review. There can be important differences between the submitted version and the official published version of record. People interested in the research are advised to contact the author for the final version of the publication, or visit the DOI to the publisher's website.
• The final author version and the galley proof are versions of the publication after peer review.
• The final published version features the final layout of the paper including the volume, issue and page numbers.

Link to publication

Download date: 04. Oct. 2023

All-Optical Packet Switching and Label Rewriting for Data Packets Beyond 160 Gb/s

Nicola Calabretta
Hyun-Do Jung
Eduward Tangdiongga
Harmen Dorren
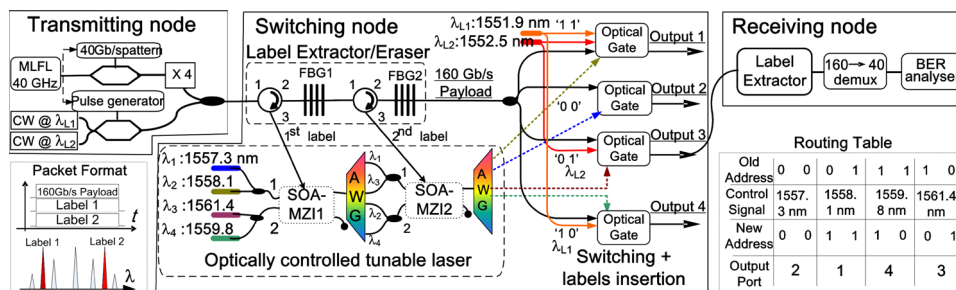
All-Optical Packet Switching and Label Rewriting for Data Packets Beyond 160 Gb/s

Nicola Calabretta, Hyun-Do Jung,
Eduward Tangdiongga, and Harmen Dorren

COBRA Research Institute, Eindhoven University of Technology, 5600 Eindhoven, The Netherlands

Abstract: In this paper, two different paradigms to realize a scalable all-optical packet switch with label swapping will be reviewed. The two paradigms are based on wavelength routing switch and space routing switch. All the functions required for switching the packets, namely, the label processor, the label rewriter, and the optical switch, are based on all-optical signal processing with no electronic control. This allows for very fast processing time and potential photonic integration of the systems. We report, for both techniques, experimental results showing the routing operation of the 160-Gb/s packets and beyond. We will discuss and compare both techniques in terms of devices and bit-rate scalability, power consumption, power penalty performance, and cascadability as key parameters for the realization of an all-optical packet switch.

Index Terms: Optical packet switching, optical signal processing, label processor, label rewriter, label swapping, wavelength converter, semiconductor optical amplifier.

1. Introduction

The exponential growth of the Internet data traffic will demand high-capacity optical networks. It might occur that high-capacity optical links will carry optical packets at data rates above 100 Gb/s using a variety of data formats such as optical time-division multiplexing (OTDM) return-to-zero data packets [1], multiwavelength optical packets with high-spectral-efficiency multilevel modulations, such as D(Q)phase shift keying, orthogonal frequency division multiplexing (OFDM), and multiple-quadrature amplitude modulation (M-QAM) [2]–[4]. On the other hand, routing of packets by today electronic circuit switching may have fundamental limits due to the speed and the scalability of multirack electronic switching fabrics and the associated power consumption by optoelectronic conversions [5]–[7].

Current networks are based on electronic circuit switching technology in combination with wavelength-division multiplexing (WDM) technology. Despite the flexibility of the electronics for processing the packet addresses, a typical electronic circuit switch requires electrical clock recovery, electrical serializer/deserializer to scale down the line rate of the optical packets (typically > 10 Gb/s) to a data rate compatible with the electronic speed (< 622 Mb/s) for processing the labels, multiplexing the packets, and switching the packets to the proper output port. With the increase of the data rate of the optical packet (above 40–100 Gb/s) and of the number of WDM channels to meet the capacity demand, electronic circuit switching may have fundamental limits due to the scalability of multirack electronic switching fabrics, as well as power consumption and dissipation required by the optoelectronic conversions [5], [6]. Moreover, packet switching operation on optical packets with high
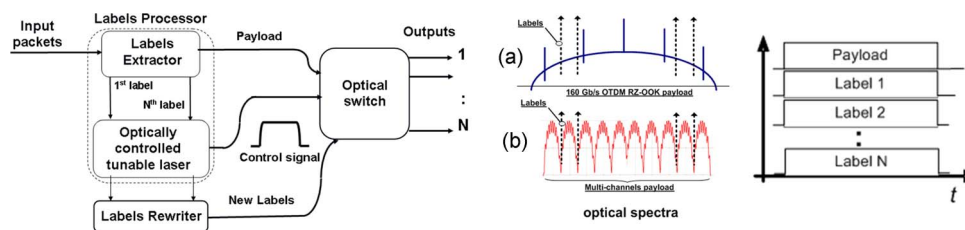
Fig. 1. All-optical packet switch configuration. (Bottom) Packet format represented in the time and spectral domain.

spectral efficiency modulation format makes the optoelectronic front ends even more complex and with larger power consumption.

All-optical packet switching has been proposed as a technology to solve the bottleneck between the fiber bandwidth (BW) and the electronic router capacity by exploiting high speed and parallel operation of all-optical signal processing. In the optical packet switch (OPS), the optical packets are processed in the optical domain without the power-hungry optoelectronic conversions. This leads to a large reduction of power consumption. Moreover, photonic integration of the OPS potentially allows for a reduction of volume, power consumption and costs. The OPS subsystem is shown in Fig. 1. In all-optical packet switches the optical packets are routed based on the address information that is encoded by the attached labels. The optical packet is stored (delayed) in the optical domain for the time required to the label processor to process the address and provide a routing signal for routing all-optically the stored packet.

Switching of the optical packets transparently in the optical domain eliminates power-hungry optoelectronic conversions [6]–[18]. However, there are several issues to be addressed for realizing such an OPS subsystem. The OPS subsystem should be able to handle optical packets with multiple data formats. This implies that both the label processor, which determines the packet destination and controls the switching fabric, as well as the optical switching fabric, should operate independently of the data format and the data rate of the packets. The OPS subsystem should be scalable, which means that the number of input/output ports is not limited by switch architecture. For instance, a large $N \times N$ switching matrix based on Clos architecture [20] can be realized starting from a $1 \times N$ switch. Essential in realizing a $1 \times N$ OPS is the implementation of a scalable label processor. Moreover, the OPS subsystem should introduce little latency to increase the node throughput.

To exploit the benefit of photonic technology to miniaturize and decrease the power consumptions of the system, photonic integration of the all-optical packet switch depends on the capability to integrate the label processor and the optical delay related to the processing time of the label processor. This imposes stringent constraints on the processing time of the label processor. Indeed, integrated delay lines using an InP photonic waveguides have around 2 dB/cm of optical losses. One centimeter of waveguide provides a delay of 100 ps. If the latency of the label processor is in the order of 1 ns, integration of such delay exhibits a total waveguide loss of 20 dB, which is impractical. Therefore, high-speed operation of the label processor (< 100 ps) is a must to allow photonic integration of the packet switch system. Moreover, scalability of the label processor with the number of labels (or the number of label bits) is also crucial. Indeed, the number of active components that can be integrated in the label processor is limited by the thermal crosstalk and heat dissipation, which can prevent photonic integration of the circuit. A method that has been introduced to minimize the number of active components in the label-processor architecture is the all-optical label swapping (AOLS) [7]. In AOLS, only few labels for routing the optical packet have to be processed at each node, thus leading to a considerable simplification of the label-processor architecture.

Several solutions were presented to implement an all-optical packet switch node. All-optical packet switch employing an all-optical label processor were investigated in [6]–[18]. Mainly these works employed optical correlators, which recognize the labels and set/reset optical flip-flops to store the information for the duration of the packet. However, as the number of addresses of the

WDM channels carried by each fiber and of the packet data rate increase, photonic integration, high-speed operation, low latency, and scalability of the label processor remain key issues to be solved. Solutions employing 2^N optical correlators and 2^N optical flip-flop to process the addresses may prevent photonic integration.

Our research focuses on the realization of an all-optical packet switching system that is scalable and suitable for photonic integration. We present two AOLS techniques that utilize all-optical signal processing to implement the label processor and the label rewriter. The two techniques are based on two different paradigms. One is based on wavelength routing switching [18] and the other one on space routing switching [19]. Both techniques employ scalable and asynchronous label processor and label rewriter capable to process optical in-band labeling addresses [18]. The label processor and label rewriter process "on the fly" the optical labels, which results in low processing time of a few hundreds of picoseconds. We report for both technique's experimental results, showing the routing operation of the 160-Gb/s packets based on the processed in-band address information and all-optical label erasing and new label insertion operation. Moreover, photonic integrated subsystems required to implement the packet switch will be presented.

The paper is organized as follows. In Section 2, we present the $1 \times N$ all-optical packet switch subsystem architecture. We introduce the packet data format and the main all-optical functions required to accomplish the AOLS, namely, the all-optical label processor, the all-optical label rewriter, and the optical switch. In Section 3, we will demonstrate the operation of the all-optical label extractor/eraser and the all-optical label processor for different modulation format and discuss the scalability to large number of labels. In Sections 4 and 5, experimental results that demonstrate the operation of the two all-optical packet switches paradigms based on wavelength routing switching and space routing switching are presented, respectively. In Section 6, we provide a comparison between the two AOLS techniques. Finally, we summarize and discuss the main results in the conclusions section.

2. All-Optical Packet Switch Architecture

Fig. 1 illustrates the all-optical packet switch based on label-swapping technique and the format of the optical packets. Generally, optical packets at high data rate B can be generated in serial by using OTDM techniques or in parallel by using N colored channels, and each channel has bit rate B/N. Both the OTDM packets and N-channels can be encoded by many modulation formats. We encode the address information of optical packets by in-band labels, i.e., the wavelengths of the labels are chosen within the BW of the payload. We have already validated this technique for 160-Gb/s OTDM packets; the labels were inserted within the spectrum of the OTDM signal [see Fig. 1(a)]. For the DPSK multiwavelength packets, we use the same label wavelengths, but they are spectrally located in the notches of the spectra of the multiwavelength payload [see Fig. 1(b)] [21]. Each label is on–off keying (OOK) encoded and has a binary value: The label value is "1" if the label is attached to the payload, and the label value is "0" if no label is attached to the payload. We encode addresses by combining different labels. Thus, by using N in-band label wavelengths, 2^N possible addresses can be encoded, which makes this labeling technique highly scalable within a limited BW. The maximum number of labels and the position of the label wavelength within the spectral lines of the payload are limited by the spectral distortion induced by the filtering process. The narrower the BW of the stop-band of the filter, the less spectral distortion there will be, and then, a power penalty will occur. Therefore, for scaling the label extractor for a larger number of labels, it is indispensable to properly design filters with a narrow BW. In [17], it was discussed that, for a 160-Gb/s OTDM payload, more than 25 labels can be inserted/extracted by using a filter with a -3-dB BW of 0.1 nm. This will lead to a very large (2^{25}) number of addresses. This was partially verified in [21], where by using fiber Bragg gratings (FBGs) with a -3-dB BW of 0.06 nm, six labels were inserted/extracted with no noticeable penalty. Note that if the payload data rate increases above 160 Gb/s (i.e., 320 or 640 Gb/s), a larger number of labels can be allocated in the payload spectrum. Thus, the proposed labeling technique scales well with the packet data rate. Other advantages of the in-band labeling are that the labels can be extracted by passive wavelength filtering. Moreover, by using a label that

has the same time duration as the payload makes the use of optical flip-flops redundant and allows handling of packets with variable lengths in an asynchronous fashion. Fig. 1 shows packets carrying different addresses and the corresponding representation in the spectral domain.

The all-optical packet switch is based on a label-swapping technique. In the label-swapping technique, the input labels have only a local meaning. The input labels are used to provide the packet's routing information. New labels should be generated and attached to the packet payload before that the packet outputs the switch. To perform the label swapping and routing of the packet, we utilize three all-optical functions, as shown in Fig. 1: all-optical label processing, all-optical label rewriting, and all-optical switching. The packet address encoded by the in-band labels is first processed by the all-optical label processor. The label processor separates the data payload from the labels. The data payload is optically delayed for the time required to the label process to provide a routing signal before being fed into the optical switches. The labels all-optically control the optically controlled tunable laser (OCTL) and label rewriter. The OCTL provides the routing signal according to the input labels. The routing signal at unique wavelength has a time duration equal to the packet time. The wavelength of the routing signal is used to drive the optical switch. Simultaneously, the label rewriter provides the new labels, which have a time duration equal to the packet duration. Moreover, the wavelengths of the new labels are selected so that they are in-band with the BW of the converted payload. The new labels are attached to the switched packet. Note that since the label processor and label rewriter operate "on the fly," the time delay required to store the payload is very short. This may allow photonic integration of the whole packet switch system. Moreover, as the routing signal and the new labels produced by the label processor and label rewriter have a time duration equal to the packet time, the presented system can handle packets with variable length.

In the next section, we present the operation principle and experimental results for different modulation formats of the all-optical label processor. Scalability of the label processor with respect to the number of labels will be also discussed.

3. All-Optical Label Processor

The all-optical label processor should provide the routing control to properly switch the optical packets to the proper output based on the packet's destination information carried by the optical labels. The all-optical label processor is shown in Fig. 1. It consists of an all-optical label extractor/eraser and an OCTL. The label extractor/eraser separates the in-band labels from the data payload. The separated labels set, for a time duration equal to the packet time, the wavelength of the optical signal generated by the OCTL. This optical signal at unique wavelength represents the routing signal. We first discuss the operation of the label extractor/eraser with different modulation formats, followed by the OCTL.

3.1. All-Optical Label Extractor/Eraser

The label extractor/eraser separates the in-band labels from the data payload. The label extractor can be implemented by optical passive filters. One possible technology to implement the label extractor is the use of (reflective) FBGs centered at the labels wavelengths. While the labels are reflected by the FBGs, the packet payload can pass through the label extractor/eraser before entering the switch. We have used narrow-BW FBGs with Gaussian profile, 98% of reflectivity, and 6 GHz at -3-dB BW to avoid significant slicing of the spectrum of the payload that may lead to distortions. The advantage of this label extractor is that the labels output in parallel so that each label can directly drive the OCTL, as discussed in detail in the next section.

The experimental setup to demonstrate the label extractor/eraser operation of packets with multiple modulation format and in-band labels is shown in Fig. 2. At the transmitter side, we generate payloads with two types of modulation formats. First, 160-Gb/s OOK payload centered at 1546 nm is generated by time-multiplexing 40-Gb/s modulated optical pulses. The 1.4-ps optical pulses make the -20-dB BW of the payload be 5 nm. Second, 12×10 Gb/s DPSK multiwavelength payload with channels from 1544.1 nm to 1548 nm spaced by 50 GHz. The optical address coupled
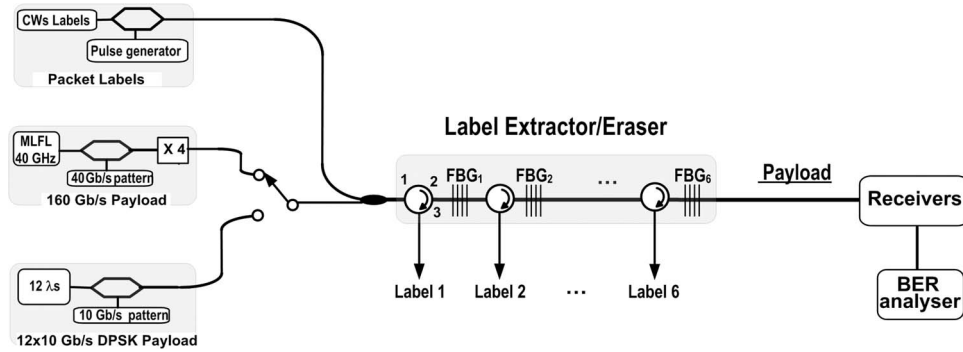
Fig. 2. Experimental setup for validating the operation of the all-optical label extractor/eraser.
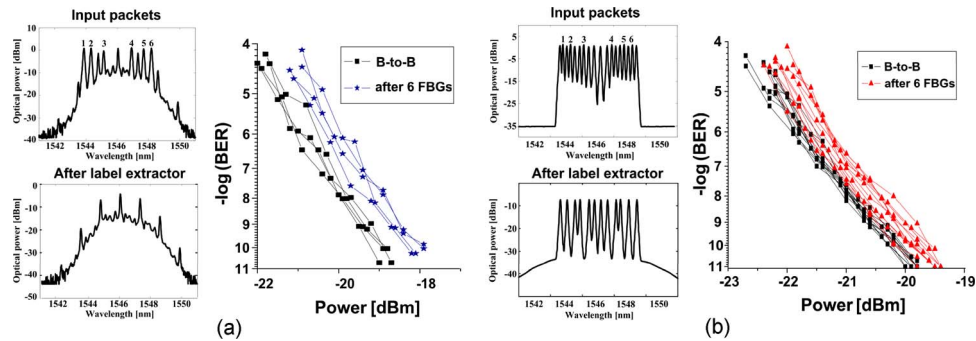

Fig. 3. Optical spectra of the packets before and after the label extractor and BER curves for (a) 160-Gb/s RZ-OOK and (b) 120-Gb/s NRZ-DPSK.

to the payloads was generated by encoding six labels with the same duration as the packet payload and with wavelengths $L_1 = 1543.88$ nm, $L_2 = 1544.36$, $L_3 = 1545.16$, $L_4 = 1546.92$, $L_5 = 1547.72$, and $L_6 = 1548.2$ nm. Note that the labels are located within the optical spectra of the two types of payload [see Fig. 3(a) and (b)]. We fed into the label extractor/eraser packets with six in-band labels and a data payload with different formats. We evaluate the quality of the payloads after filtering the in-band labels. The optical spectra of the packets before and after the label extractor and the bit error rate (BER) measurements are shown in Fig. 3. For 160-Gb/s RZ-OOK, error-free operation with 0.6-dB power penalty was measured [see Fig. 3(a)]. Similarly, less than 0.4 dB of power penalty was measured for the 12×10 Gb/s DPSK format. Those results indicate that in-band labeling can be used with different payload formats without compromising the signal quality.

Despite those successful results, the label extractor/eraser based on FBGs is not suitable for photonic integration. A possible photonic integrated device that can operate as a label extractor/eraser is a microring resonator with a pass-trough and a drop port. By exploiting the narrow BW of the drop port and the flat all-pass band of the pass-through port, simultaneous error-free label extraction and label erasing has been performed without noticeable pulse distortion. The experimental setup employed to demonstrate the microring-based label extractor/eraser is shown in Fig. 4. The packet format is the same as the one shown in Fig. 1. We employ two in-band labels at $\lambda_{L1} = 1549.45$ nm and $\lambda_{L2} = 1553.85$ nm and a 160-Gb/s RZ-OOK payload for the demonstration. The label extractor/eraser consists of a pigtailed vertically coupled microring resonator fabricated in the Si3N4/SiO2 materials system [22] (high-contrast materials system, $\Delta n \approx 0.55$), with a pass-through port and a drop port, as shown in Fig. 4(a). The transfer function of the pass-through port is reported in Fig. 4(b). The free spectral range (FSR) of the periodic stop-bands is 4.4 nm. A magnification of one of the stop-band is shown in Fig. 4(c). The measured -3-dB BW was 0.16 nm, and the flatness of the pass-band was $+/-0.4$ dB. The stop-bands at multiple FSR are
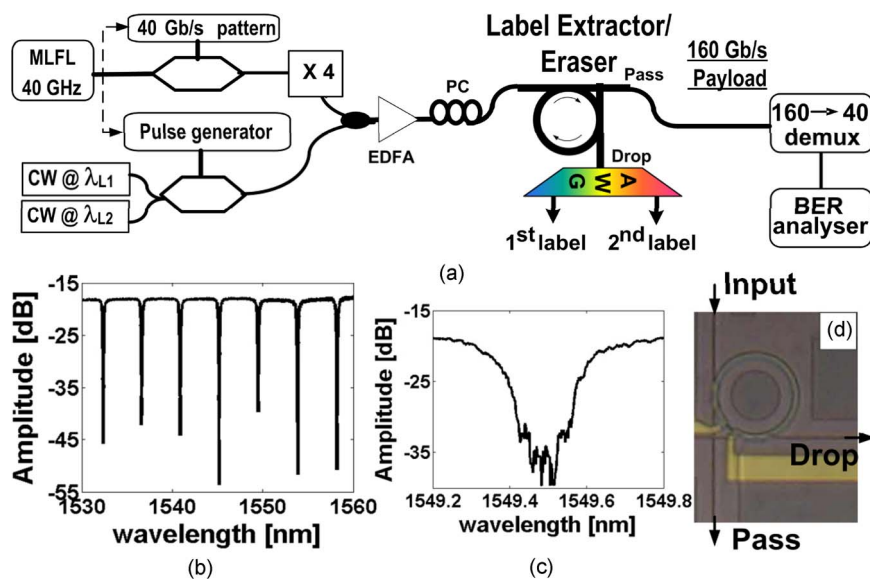
Fig. 4. (a) Experimental setup. (b) Transfer function of the pass-through. (c) Magnification of one of the stop-band. (d) SEM of the microring resonator employed in the experiments.
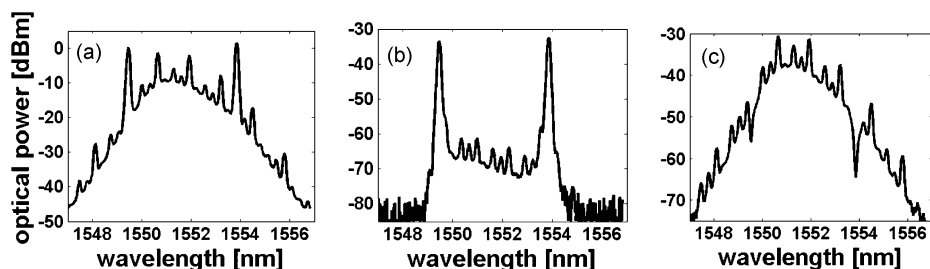

Fig. 5. Measured optical spectra. (a) Optical packets at the input of the label extractor. (b) Optical spectra of the two labels at drop port output. (c) Optical spectrum of the 160-Gb/s payload after the pass-through port.

designed to be at the wavelengths matching the labels wavelengths. Therefore, the labels wavelengths are filter out at the drop port, while the wavelength payload is output to the pass-through port. The two labels at wavelength λ_{L1} and λ_{L2} are output from the drop port and then separated by an arrayed waveguide grating (AWG) filter ready to be fed into the OCTL. In Fig. 5, the optical spectra measurements with resolution BW of 0.06 nm at the drop and pass-through ports are reported. The optical spectrum of the input packet before the label extractor is shown in Fig. 5(a). The optical spectrum at the output of the drop port and the pass-through output port are reported in Fig. 5(b) and (c), respectively. More than 25 dB of separation between the labels and the optical payload was measured. The eye diagrams of the original input 160-Gb/s data payload and of the 160-Gb/s payload after the label extractor/eraser are reported in Fig. 6(a) and (b). An optical sample oscilloscope with a 700 GHz of BW was employed to record the eye diagrams of the 160-Gb/s pulses. Very small degradation and broadening of the pulses is observed after the label extraction. The measured pulse-width broadening was 0.4 ps. The measured RMS time jitter was 212 fs for the pulses after the label extractor/eraser, which results in an increase of 40 fs, compared with the 173 fs of the input 160-Gb/s payload pulses. To quantify the performance of the label extractor/eraser, BER measurements are reported in Fig. 6(c). The BER measurements were performed in a static operation by time-quadrupling 40-Gb/s pseudo-random binary sequence (PRBS) $2^{31} - 1$ data payload. The resulting 160-Gb/s data payload after the label extractor/eraser is amplified and time-demultiplexed from
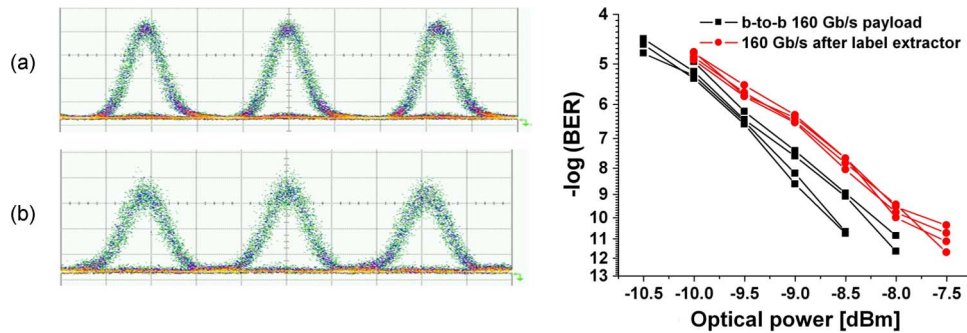
Fig. 6. (a) Eye diagram of the input 160-Gb/s payload. (b) Eye diagram of the 160-Gb/s payload after the label extractor/eraser. The time scale is 2 ps/div. (c) BER measurements before and after the label extractor/eraser.
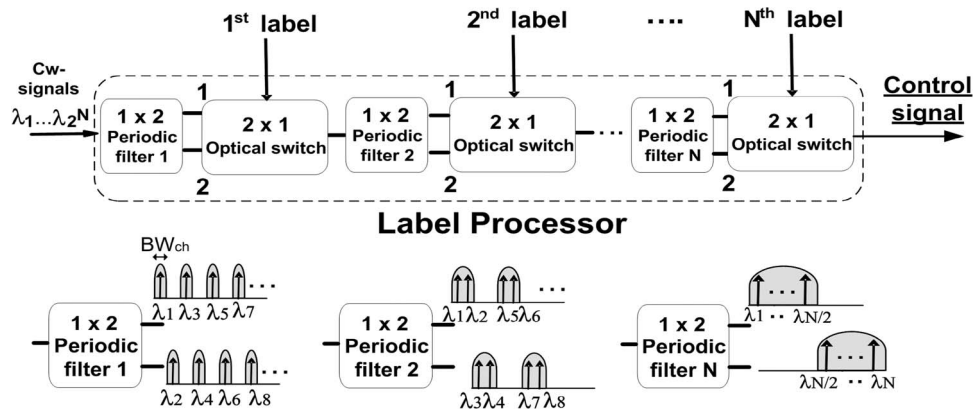

Fig. 7. Schematic of the label processor. Details of the optical period filters employed in the device are shown at the bottom.

160 Gb/s to 40 Gb/s by using an electrically clocked electro-absorption modulator that creates a 5-ps switching window with a periodicity of 25 ps. The resulting 40-Gb/s data is then detected by a 40-Gb/s detector and analyzed by using a BER tester. As a reference, we report the BER curve of the back-to-back (b-t-b) 160-Gb/s payload. The BER curve of the 160-Gb/s payload after the label extraction/eraser shows error-free operation with a limited power penalty of around 0.5 dB. The low power penalty can be ascribed to the additional amplified spontaneous emission noise introduced by the amplification stage required to compensate the total loss of the label extractor/extractor. This work demonstrates the feasibility of using a passive silicon-nitride microring add/drop resonator for photonic integration of the label extractor/eraser.

3.2. Label Processor by the OCTL

The schematic of the OCTL is illustrated in Fig. 7. The optical power of the extracted labels is used to drive the label processor. The label processor receives also as input 2^N continuous waveform (CW) bias signals at different wavelengths $\lambda_1, \ldots, \lambda_2^N$. The label processor consists of a cascaded of N pairs of periodic filter and optical switch. The periodic filter has one input and two outputs. The optical switch has two inputs and one output. The two outputs of the periodic filter have complementary wavelength transfer functions, as shown in Fig. 7. Moreover, each of the N periodic filters has different period, as also shown in Fig. 7. In particular, the BW of the ith filter is equal to $\mathrm{BW}_i = 2^{(i-1)} \times \mathrm{BW}_{ch}$, with $i = 1, \ldots, N$ and BW_{ch}, which is the BW of the single CW signal. Each 1×2 periodic filter separates (in wavelength) half of the input CW signal to output port 1 and the other half of the input CW signals at the output port 2. The 2×1 optical switch selects the CW signals of
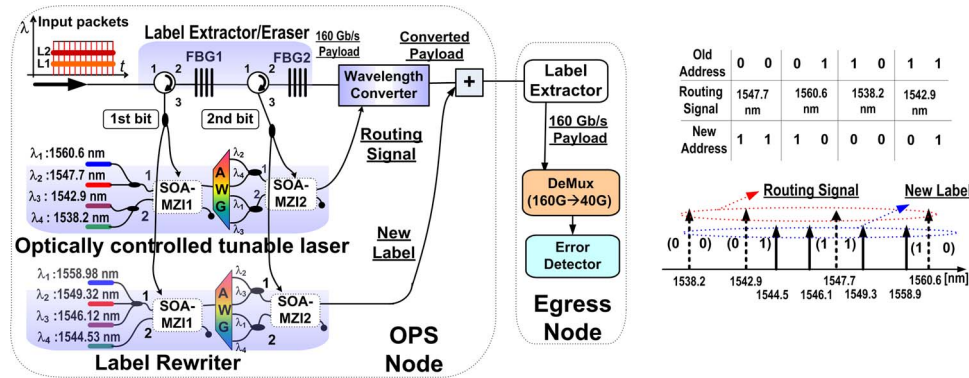
Fig. 8. Experimental setup employed the AOLS based on wavelength routing switch.

port 1 or port 2 based on the value of the label information. Therefore, the output of each pair of periodic filter and optical switch consists of half the number of CW signals. Thus, after the first stage, the 2^N CW signals becomes $2^N/2 = 2^{N-1}$. Therefore, after cascading N pairs in which each optical switch is driven by the corresponding label, a distinct CW signal is selected. This CW signal at distinct wavelength has a time duration equal to the packet time duration and represents the routing signal to which the payload will be converted. Note that the processing is performed entirely in the optical domain. As no synchronization is required in the scheme, and since the routing signal at the label processor output has the same duration as the packet payload, the system can handle packets with variable lengths.

4. All-Optical Packet Switch Based on Wavelength Routing Switch

We have demonstrated that the all-optical label processor produces, based on the label information, a routing signal for controlling all-optically the packet switch. Referring to the schematic of the OPS in Fig. 1, two distinct paradigms can be employed to perform an all-optical packet switch, namely, wavelength routing switching and space routing switching. In this section, we discuss the OPS based on wavelength routing switching.

To perform the label swapping and routing of the packet, we utilize the schematic shown in Fig. 8. The input packet is first processed by the label processor, as discussed in Section 2. For each input label combination, the label processor provides a routing signal according to the input labels. The routing signal at a unique wavelength has a time duration equal to the packet time. The wavelength of the routing signal represents the central wavelength at which the 160-Gb/s data payload will be converted by means of wavelength conversion [23], [24]. Simultaneously, the label rewriter provides the new labels, which have a time duration equal to the packet duration. The principle of operation of the label rewriter is similar to the label processor. In the case of the label rewriter, the CW signals and the periodic filters are set to provide the new label combinations according to the self-routing table shown in Fig. 8. The wavelengths of the CW signals are set to be in-band with the switched payload (the central wavelength of the payload is set by the label processor). Thus, for a given old-label combination, the routing signal is provided by the label processor, and the new labels are provided by the label rewriter. Note that the case of new labels "0 0," means no optical signals at the labels wavelength, while in the case of new labels "1 1," the label rewriter should provide two CW signals at distinct wavelengths. According to the swapping table in Fig. 8, for a given old label combination, the routing signal is provided by the label processor, and the new labels at wavelengths in-band with the switched payload are provided by the label rewriter. As an example, if a packet with labels "0 1" enters the packet switch (see the self-routing table in Fig. 8), the payload is converted at 1560.6 nm, and a signal at 1558.9 nm, in-band with the payload spectrum, that represents the new labels "1 0" is obtained at the label-rewriter output. The new labels are coupled to the converted payload so that at the packet switch output, the switched packet contains the new
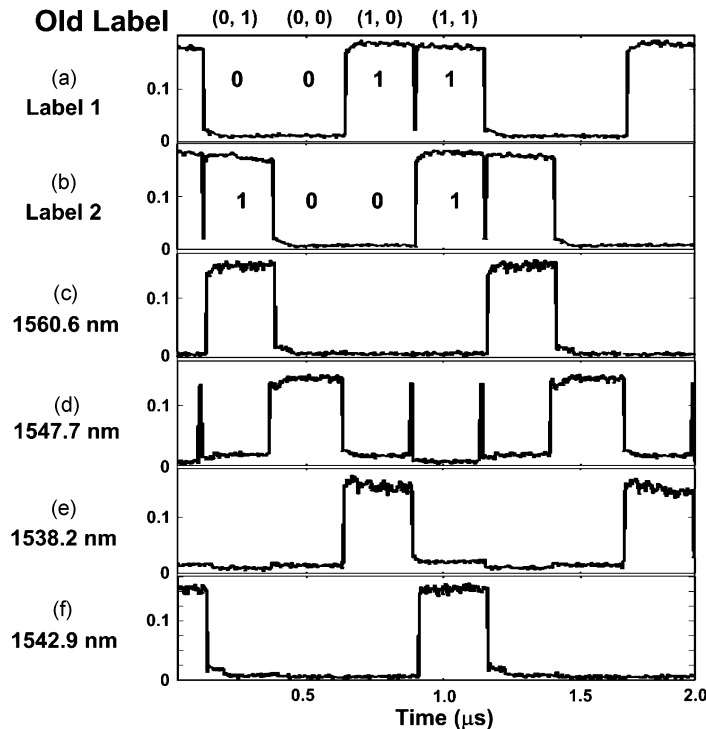
Fig. 9. Measured traces. (a) and (b) Extracted labels. (c)–(f) Output traces of the label processor.

in-band label information. The packet with the new labels is routed by means of an AWG to distinct output ports of the packet switch.

Fig. 8 shows the experimental setup employed to investigate a 1 × 4 all-optical packet switch based on wavelength routing technique. We processed four packets with two labels with pattern of "0 0," "0 1," "1 0," "1 1" to cover the all possible combinations. The packet format employed in the experiments is similar to the one used in the label-processor experiment. We set the CW signals according to the label-swapping table reported in Fig. 8. The label bits extracted by the label extractor are shown in Fig. 9(a) and (b). In the experiment, we used two labels with the wavelengths of $\lambda_{L1} =$ 1551.9 nm and $\lambda_{L2} =$ 1552.5 nm, which are within the 20-dB optical BW of the packet payload. Fig. 11(b) shows the spectrum of the payload signal after label extraction. As compared with Fig. 11(a), the label was erased. Based on two-label combination and according to the self-routing table, the label rewriter gave four sets of new labels. The label-processor output traces are shown in Fig. 9(c)–(f), while the label-rewriter output traces are shown in Fig. 10(c)–(f). It can be observed that for input labels combination "0 1," the label processor produces the routing signal at 1560.6 nm [see Fig. 9(c)], while the label rewriter produces the new labels "1 0" represented by the signal at wavelength 1558.9 nm [see Fig. 10(c)]. For the old label combination "0 0," a routing signal at 1547.7 nm is obtained [see Fig. 9(d)], and the new labels "1 1" are represented by signals at wavelength 1546.1 nm and 1549.3 nm [see Fig. 10(d)–(e)]. For the combination "1 1," a routing signal at 1542.9 nm [see Fig. 9(f)] and new labels "0 1," represented by the signal at wavelength 1544.5 nm [see Fig. 10(f)], was obtained. Finally, the combination "1 0" produces a routing signal at 1538.2 nm [see Fig. 9(e)] and a new label "0 0" that means no signals. The routing signal is used in the wavelength converter to route the packets in a wavelength routing switch configuration, while the new labels from the label rewriter were combined with the 160-Gb/s converted payload. Note that the wavelengths of the new labels are chosen to be in-band with the converted payload. The output of the label processor (and label rewriter) for different old label combinations consists of routing signals with time duration equal to the payload. Note that only for an address "00," the output trace shown in Figs. 9(d), 10(d), and 10(e) presents also some pulses in correspondence of
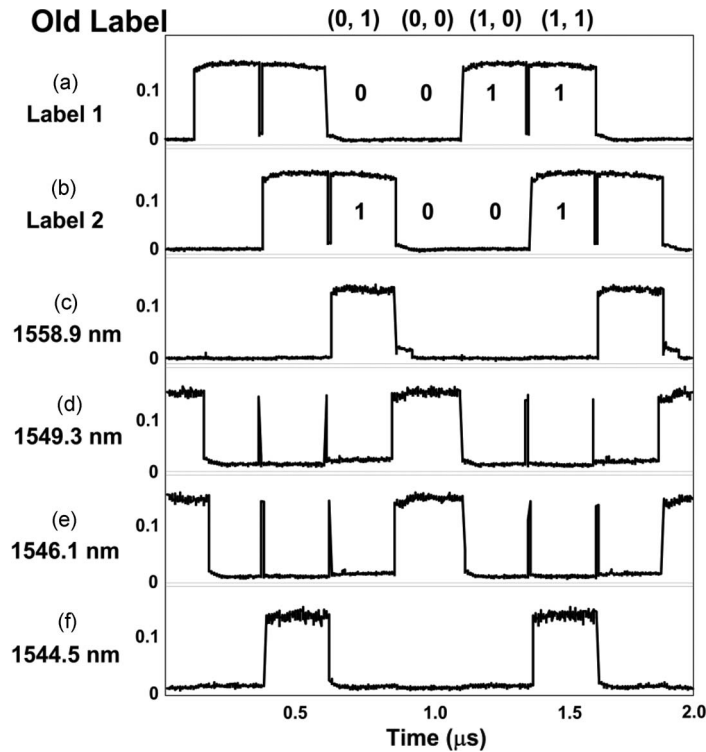
Fig. 10. Measured traces. (a) and (b) Extracted labels. (c)–(f) Output traces of the label rewriter.
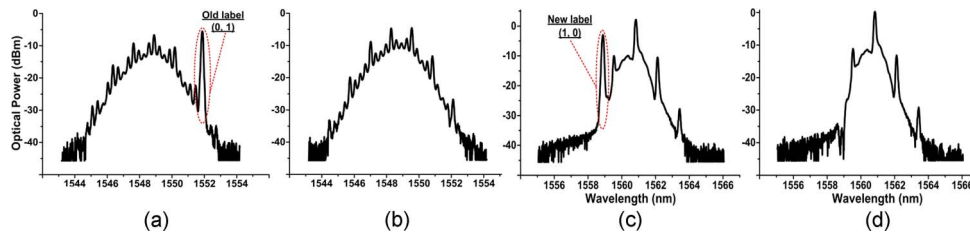

Fig. 11. Optical spectra recorded at (a) input packets, (b) after the label extractor/eraser, (c) wavelength-converted payload with the new label, and (d) after the label extractor at the receiver side.

the packet guard time. Those pulses, with a time duration equal to the packets' guard time, are indeed generated during the guard time (which also provides a "00" combination). However, when the wavelength converted between the packet payload and the routing signal takes place, those pulses being in correspondence with the packet's guard time and due to the noninverting operation of the wavelength converter, those pulses will be suppressed and, thus, do not affect the system performances, as confirmed by the BER measurements. To quantitatively investigate the all-optical packet switch, the switched packet was fed into a label extractor/eraser, and the resulting 160-Gb/s payload was evaluated. Fig. 12 shows the BER performance at different position of the two-node system. The BER measurements were performed in a static operation by using a 160-Gb/s PRBS $2^{31} - 1$ data payload and fixing one address [old label "0 1"; see spectrum in Fig. 11(a)]. The label extractor causes a penalty of less than 0.5 dB compared with the b-t-b payload. After the wavelength conversion, error-free operation was obtained with a penalty of 5.5 dB. As a reference, we also reported on the 160-Gb/s b-t-b wavelength converted, which has a 4-dB power penalty. The additional 1.5-dB penalty compared with 160-Gb/s b-t-b wavelength conversion can be ascribed to the pulse broadening by the label extractor which affects the wavelength-conversion performance. The switched packet with the new label (1, 0) [see spectrum in Fig. 11(c)] was then evaluated. The
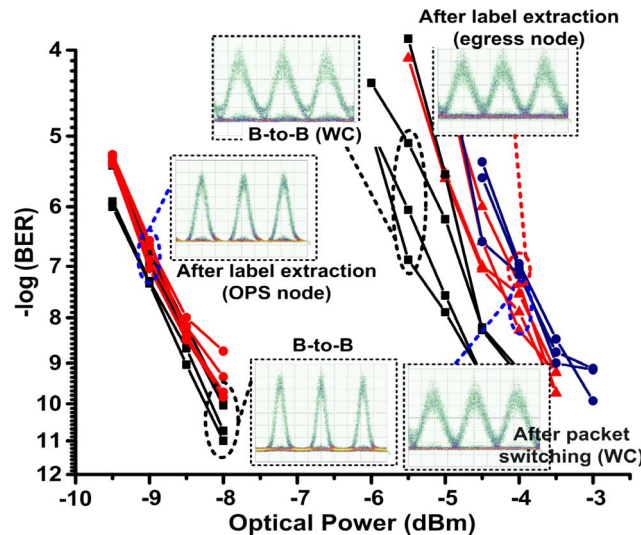
Fig. 12. BER curves and eye diagrams at different points of the system. Time scale is 2 ps/div.
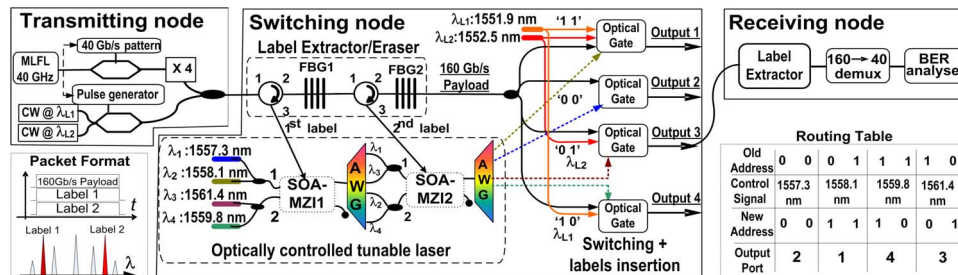

Fig. 13. Experimental setup and packet format. The routing table is also reported.

optical spectrum of the packet after the label extractor 2 is reported in Fig. 11(d). The power penalty after the label extractor is 0.5 dB. This results in a limited power penalty caused by the extraction/ insertion of the new labels. These results validate the label-rewriting operation. Note that generally, in the label rewriter, the number of CW signals required is greater than in the case of the label processor. For a large number of CW signals, the total optical power injected into the SOA-MZI should be decreased to avoid impairments due to the high saturation of the SOA. This results in a decrease in the OSNR of the selected new labels. We have measured that the OSNR decreases from 38 dB to 32 dB when four or 16 CW signals were injected in the SOA-MZI, respectively. This means that the OSNR decreases with 3 dB after doubling the number of input CW signals. However, as new labels are rewritten at each node, the required OSNR of the new labels should be large enough only to guarantee the transmission between two nodes.

5. All-Optical Packet Switch Based on Space Routing Switch

In this section, the OPS based on space routing switching is discussed. The schematic of the 1×4 all-optical packet switch is shown in Fig. 13. The data packet is similar to the one employed in the wavelength routing switch. The packet payload consists of a 6-ns data burst. The guard time between the packets is 400 ps. We encode four addresses by using two in-band labels at $\lambda_{L1} = 1551.9$ nm and $\lambda_{L2} = 1552.5$ nm. The AOLS consists of a label processor and four optical gates as space switching and label rewriting. Note that the label rewriting is performed directly by the optical gates. The input packets are first processed by the label processor that provides the control signal for one of the SOA-MZI-based optical gates. These optical gates have two functions.
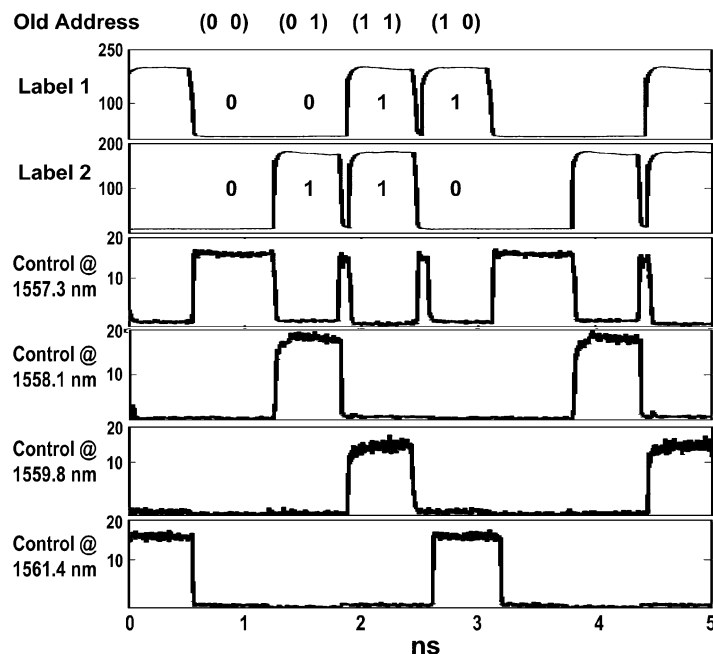
Fig. 14. (a) and (b) Extracted labels. (c)–(f) Output traces of the label processor. Vertical scale is in megavolts.

First, they route the packet payload according to the routing table in Fig. 13. Second, they rewrite the new labels.

Fig. 13 shows the routing table for the new addresses. For example if the old address was "10," the label processor generates a control signal with a wavelength of 1561.4 nm. It is also visible from the routing table that the new address is "01." This means that the new cw label has a wavelength of 1552.5 nm (which is in band with the packet payload). Both the payload and the new cw label are fed simultaneously into the SOA–MZI gate that is controlled by the label-processor output. If a control signal is present, the SOA-MZI gates both the packet payload, together with the new label, to the output.

Conversely, the gate output is blocked. The operation of the gate guarantees that the payload and the new label have the same duration at the gate output.

The experimental setup to demonstrate the 1 × 4 AOPS with label-swapping functionalities is shown in Fig. 13. We processed four packets with addresses "0 0," "0 1," "1 0," and "1 1" to cover all possible combinations. The extracted labels are shown in Figs. 14(a) and 15(b), while the payload is shown in Fig. 15(a). The label-processor output traces are shown in Fig. 14(c)–(f). The dynamic extinction ratio was 13 dB. The label processor output was amplified by an SOA and distributed to the 4 optical gates by means of an AWG. The optical power of the control signal at the optical gate was −3.3 dBm. Fig. 15(b)–(e) report the traces of the switched payload and the inserted new labels at different output ports. We also report in the insets the optical spectra showing the switched payload and the new labels. To evaluate the performance, the switched packets are fed into a receiving node consisting of a label extractor (only the payload is evaluated), a 160-to-40-Gb/s demux, and a 40-Gb/s detector. Fig. 16 shows the BER curves. As a reference, we report the BER curve of the b-t-b 160-Gb/s payload. The BER curve of the switched packet at Output 2 (no new label inserted) shows error-free operation with 1 dB of power penalty. We also report the BER curve of the switched packet at Output 3, in which a new label ("01") is inserted. An additional power penalty of < 0.5 dB was measured, compared with the case without label insertion.

This indicates that the switch with label rewriting introduces very small penalties. As a final result, we report, in Fig. 16, the eye diagrams of the b-to-b payload and the switched payload at 320 Gb/s.
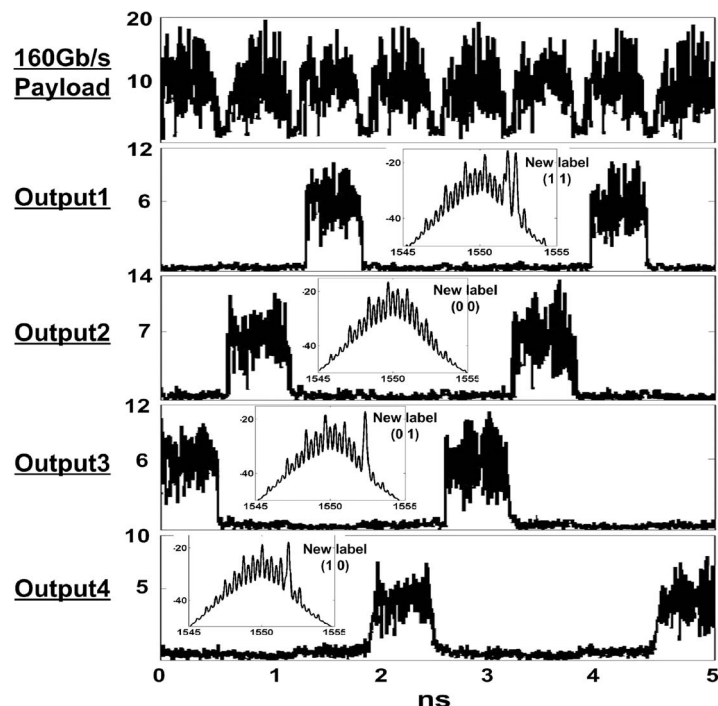
Fig. 15. (a) 160-Gb/s payload. (b)–(e) Output traces of the AOPS. The vertical scale is in mV.
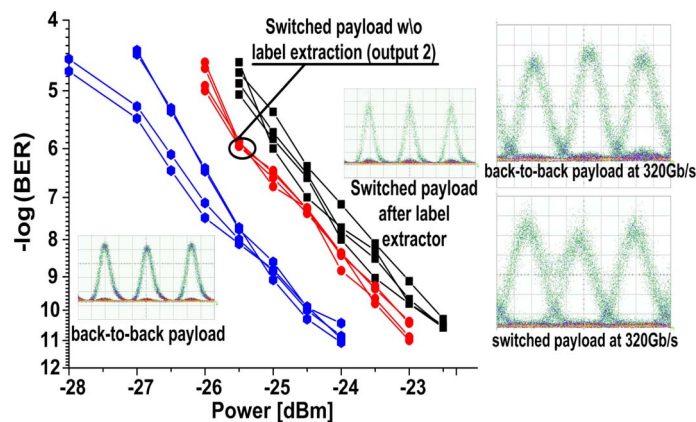
Fig. 16. BER curves. Time scale eye diagrams 1 ps/div.

Although the eye diagram gives only qualitative information, the clear open eye suggests that error-free operation at 320 Gb/s is feasible.

6. Performance Comparison of the Two AOLS Techniques

In this section, we compare both techniques in terms of devices and bit-rate scalability, processing time, node cascadability, and data-format transparency as key parameters for the realization of an all-optical packet switch.

6.1.1. Device scalability

The AOLS should be scalable in terms of number of input and output ports and number of components. It is important that these large AOLS can still be controlled with a limited amount of

signals and that the number of control signals scales efficiently with the number of input and output ports. Finally, it is important that the switch introduces low signal degradation. The label processor (and label rewriter) requires $\log_2 N$ active components (N is the number of packets' addresses). The AOLS based on wavelength routing switch then requires $2 \times (\log_2 N) + 1$, including the wavelength converter. In the AOLS based on space switch, the number of components is $\log_2 N + N$, including the N optical switches employed for switching and label rewriting. As the number of ports N increases, wavelength routing switch seems to be the best choice. However, from the point of view of signal degradation, it should also be considered that in the wavelength-routing technique, the routing signal generated by the OCTL represents the wavelength at which the packet will be converted. In the space routing switch, the OCTL output is employed as the control signal of the optical gates. Therefore, the high quality (high OSNR) of the OCTL output is very important in the wavelength-routing switch technique, while it is much more relaxed in the space-routing switch. For what concerns the scalability limit imposed by the OSNR degradation, since the losses of the AWG (around 3–4 dB) employed in the OCTL can be compensated by the amplification provided by the SOAs in the MZI-switches, the OSNR is expected to be reduced steeply after the first SOA-MZI switch, but after that, it degrades gradually. The calculation depends on the amplifier noise figure, the input optical power of the CW signals, and the gain of the amplifier [25]. As a reference, in a recirculation buffer containing four cascaded SOA [26] and with a totally compensated loop losses, an OSNR of 26 dB was measured after eight recirculation loops, which corresponds to 32 cascaded SOAs. Considering that the SOAs employed in [26] are shorter than the one required in the MZI-SOA based switch, OCTL with eight cascaded optical switches is reasonable, which results in a potential processing of 2^8 addressed.

6.1.2. Bit-rate scalability

The AOLS should be able to operate at a data rate beyond 160 Gb/s. For a bit rate beyond 160 Gb/s, the space-routing-switch technique outperforms the wavelength routing switch one mainly because it is capable of operating the wavelength converter with a data rate beyond 160 Gb/s with acceptable power penalty. Error-free operation was attained in both techniques. However, in the space switching technology (see Section 4), the penalty was 1.5 dB, compared with the BER measured in a b-t-b configuration. It is expected that at higher bit rate, this penalty will increase but should be acceptable for cascadability of the AOPS. On the other hand, more than 5 dB of power penalty was measured for the wavelength-routing-switch technique. This value will even be higher at a data rate beyond 160 Gb/s.

6.1.3. Processing time of the AOLS

The processing time of the AOLS in the two techniques is mainly determined by the processing time of the label processor. We have demonstrated the label processor by using semiconductor-based MZI optical switches that are suitable for photonic integration and can operate at data rates up to 40 Gb/s. This allows a total label processing time of a few hundreds of picoseconds. Having a low processing time is essential to allowing the photonic integration of the whole packet switch. The system was demonstrated with two labels. For a larger number of labels, a number of cascaded SOA-MZI switches and filters proportional to the number of labels are required. The typical length of SOA-MZI switch and the AWG is around 2.5 mm. This means that for each label, the photonic chip increases in length 3–4 mm. If we consider eight cascaded SOA-MZI switches, this leads to a length for the label processor of around 3 cm, which results in a latency of around 300 ps.

6.1.4. Node cascadability

Cascadability of the AOPS is mainly limited by the power penalty introduced by the switching technique. In the AOPS based on wavelength routing switch, the measured BER penalty was 6.5 dB (see Section 3), of which 5 dB is due to the wavelength-converter operation. In the space switch, we have recorded a penalty of 1.5 dB (see Section 4). The low power penalty allows for the cascading of the AOPS for several nodes before that of the accumulated nonlinearities and degradation of the

OSNR. Those considerations lead to the preference the AOPS based on space switching for multihop operation. However, more in depth analysis is currently under investigation by using numerical tools. A possible solution for improving the cascadability of the AOPSs is the introduced after the switch (or after a number of hops) of an optical regenerator. Note that we have only considered the power penalties induced by the switching technique. Inserting/extracting a certain number of in-band labels will also introduce a power penalty due to the spectral filtering and distortion. If the number of labels is very large, the power penalty induced by filtering the in-band labels could ultimately limit the cascadability of the system. In the label-swapping technique, only a few labels for routing the optical packet have to be processed at each node. If we consider the results reported in Section 2 that inserting/extracting six labels introduces a limited penalty of 0.6 dB, the power penalty introduced by filtering the in-band labels is negligible in comparison with the one induced by the switching technique.

6.1.5. Data format transparency

With this, it is meant that the switch should switch any data format and should be not restricted to, for instance, only to OOK. The switch should be able to handle any data format, including multilevel modulations (BPSK and QPSK), QAM, and OFDM. In Section 3, experimental results have shown that label extraction of in-band labels, and thus the label processor, can operate with different payload formats. Once the labels are separated by the payload, the labels are processed by the OCTL. In the space-routing switch, the payload is broadcast and selected by the SOA-MZI switches. This scheme then is inherently data-format transparent. Instead, in the wavelength-routing-switch technique, wavelength conversion transparent from a different data format is required. Although, in this work, we have used a wavelength converter that operates only with RZ OOK data packets, the transparent wavelength converter based on four-wave mixing in SOA [27], [28], high-nonlinear fiber [29], [30], and periodically poled lithium niobate [31], [32] can be a possible solution to implementing a data format transparent wavelength-routing switch.

6.1.6. Power consumption

It is important that these large AOLS can consume a limited amount of power. The AOLS based on a wavelength-routing switch requires $2 \times (\log_2 N) + 1 + 2N$ active components, including the label processor/label rewriter, the lasers involved in the label processor and the label rewriter, and the wavelength converter. The AOLS based on space switch requires $\log_2 N + 2N + N$ active components, including the label processor, the lasers required by the label processor and in the rewriting process, and the N optical switches. Each active switch requires around 1 W of power. Therefore, if we consider a switch with 64 ports operating at 160 Gb/s (total throughput of 10 Tb/s), the wavelength-routing switch requires 141 W (141 × 1 W), while 198 W (198 × 1 W) are consumed by the space-routing-switch technique. It seems clear that in terms of power consumption, the wavelength-routing switch seems to be the best choice.

It is interesting to note that the power consumed by the state-of-the-art 40-Gb/s transceiver employed in current electronic circuit switching is 100 W [33]. To build a switch with a throughput of 10 Tb/s, more than 250 transceivers, with a total power of 25 kW, are required only for converting the optical packets to the electrical domain and back to the optical domain. Those values clearly indicate that AOLS can reduce the power consumption in packet switches with two orders of magnitude with respect to their electronic counterparts.

7. Conclusion

We have demonstrated two paradigms to implement 1 × 4 OPS based on the label-swapping technique. All the required functions to switch the packets and to rewrite the new labels have been implemented in an all-optical manner. We employed a scalable labeling technique where by combining N in-band labels, whose wavelengths are within the BW of the payload, we can encode up to 2^N possible addresses within a limited BW. The label-processing technique can operate with different modulation formats and requires only N active devises to process "on the fly" the 2^N

addresses, which makes this technique scalable with the number of addresses. Moreover, being that the labels are in-band and with a time duration equal to the packet payload, the label processor does not require all-optical flip-flop, operates in asynchronous fashion, and can handle packets with variable lengths.

We have presented experimental results that validate the operation of the packet switch by using a two-label address. We have experimentally measured that label erasing and the new label insertion operation introduces only 0.5 dB of power penalty. Error-free packet switching operation at 160 Gb/s has been obtained in the experiments with both techniques. For the AOLS based on the wavelength-routing switch, the power penalties were 6.5, while for the space-routing switch, we have measured a power penalty of 1.5 dB. These results indicate that the label-swapping technique based on the space-routing switch can be potentially utilized to devise a multihop packet-switched network.

Acknowledgment

References

[1] C. Schmidt-Langhorst, R. Ludwig, D.-D. Gro, L. Molle, M. Seimetz, R. Freund, and C. Schubert, "Generation and coherent time-division demultiplexing of up to 5.1 Tb/s single channel 8-PSK and 16-QAM," presented at the Optical Fiber Commun. Conf., San Diego, CA, 2009, PDPC6.

[2] A. H. Gnauck, G. Charlet, P. Tran, P. Winzer, C. Doerr, J. Centanni, E. Burrows, T. Kawanishi, T. Sakamoto, and K. Higuma, "25.6-Tb/s C+L-band transmission of polarization-multiplexed RZ-DQPSK signals," presented at the Optical Fiber Commun. Conf., Anaheim, CA, 2007, PDP19.

[3] X. Zhou, J. Yu, M.-F. Huang, Y. Shao, T. Wang, P. Magill, M. Cvijetic, L. Nelson, M. Birk, G. Zhang, S. Ten, H. B. Matthew, and S. K. Mishra, "32 Tb/s (320× 114 Gb/s) PMD-RZ-8QAM transmission over 580 km of SMF-28 ultra-low-loss fiber," presented at the Optical Fiber Commun. Conf., San Diego, CA, 2009, PDPB4.

[4] H. Takahashi, A. Al Amin, S. L. Jansen, I. Morita, and H. Tanaka, "DWDM transmission with 7.0-bit/s/Hz spectral efficiency using 8 × 65.1-Gb/s coherent PDM-OFDM signals," presented at the Optical Fiber Commun. Conf., San Diego, CA, 2009, PDPB7.

[5] R. S. Tucker, "Optical packet-switched WDM networks: A cost and energy perspective," presented at the Optical Fiber Commun. Conf., San Diego, CA, 2008, OMG1.

[6] S. J. B. Yoo, "Optical packet and burst switching technologies for future photonic Internet," *J. Lightw. Technol.*, vol. 24, no. 12, pp. 4468–4492, Dec. 2006.

[7] D. J. Blumenthal, "Optical packet switching," in *Proc. LEOS*, 2004, vol. 2, pp. 910–912.

[8] J. J. V. Olmos, J. Zhang, P. V. Holm-Nielsen, I. T. Monroy, V. Polo, A. M. J. Koonen, C. Peucheret, and J. Prat, "Simultaneous optical label erasure and insertion in a single wavelength conversion stage of combined FSK/IM modulated signals," *IEEE Photon. Technol. Lett.*, vol. 16, no. 9, pp. 2144–2146, Sep. 2004.

[9] D. Klonidis, C. T. Politi, R. Nejabati, M. J. O'Mahony, and D. Simeonidou, "OPSnet: Design and demonstration of an asynchronous high-speed optical packet switch," *J. Lightw. Technol.*, vol. 23, no. 10, pp. 2914–2925, Oct. 2005.

[10] B. R. Koch, Z. Hu, J. E. Bowers, and D. J. Blumenthal, "Payload-envelope detection and label-detection integrated photonic circuit for asynchronous variable-length optical packet switching with 40-Gb/s RZ payloads and 10-Gb/s NRZ labels," *J. Lightw. Technol.*, vol. 24, no. 9, pp. 3409–3417, Sep. 2006.

[11] J. P. Wang, B. S. Robinson, S. A. Hamilton, and E. P. Ippen, "Demonstration of 40-Gb/s packet routing using all-optical header processing," *IEEE Photon. Technol. Lett.*, vol. 18, no. 21, pp. 2275–2277, Nov. 2006.

[12] F. Ramos, E. Kehayas, J. M. Martinez, R. Clavero, J. Marti, L. Stampoulidis, D. Tsiokos, H. Avramopoulos, J. Zhang, P. V. Holm-Nielsen, N. Chi, P. Jeppesen, N. Yan, I. T. Monroy, A. M. J. Koonen, M. T. Hill, Y. Liu, H. J. S. Dorren, R. Van Caenegem, D. Colle, M. Pickavet, and B. Riposati, "IST-LASAGNE: Towards all-optical label swapping employing optical logic gates and optical flip-flops," *J. Lightw. Technol.*, vol. 23, no. 10, pp. 2993–3011, Oct. 2005.

[13] M. Takenaka, M. Raburn, K. Takeda, and Y. Nakano, "All-optical packet switching by MMI-BLD optical flip-flop," presented at the Optical Fiber Commun. Conf., Anaheim, CA, 2006, OThS3.

[14] H. J. S. Dorren, M. T. Hill, Y. Liu, N. Calabretta, A. Srivatsa, F. M. Huijskens, H. de Waardt, and G. D. Khoe, "Optical packet switching and buffering by using all-optical signal processing methods," *J. Lightw. Technol.*, vol. 21, no. 1, pp. 2–12, Jan. 2003.

[15] P. K. A. Wai, L. Y. Chan, L. F. K. Lui, L. Xu, H. Y. Tam, and M. S. Demokan, "1 × 4 all-optical packet switch at 10 Gb/s," *IEEE Photon. Technol. Lett.*, vol. 17, no. 6, pp. 1289–1291, Jun. 2005.

[16] P. Seddighian, V. Baby, C. Habib, L. R. Chen, L. A. Rusch, and S. LaRochelle, "All-optical swapping of spectral amplitude code labels for packet switching," in *Proc. Photon. Switching*, San Francisco, CA, 2007, pp. 143–144.

[17] J. Herrera, O. Raz, E. Tangdiongga, Y. Liu, C. H. Mulvad, F. Ramos, J. Marti, G. Maxwell, A. Poustie, M. T. Hill, H. de Waardt, G. D. Khoe, A. M. J. Koonen, and H. J. S. Dorren, "160-Gb/s all-optical packet switching over a 110-km field installed optical fiber link," *J. Lightw. Technol.*, vol. 26, no. 1, pp. 176–182, Jan. 2008.

[18] N. Calabretta, H.-D. Jung, J. Herrera, E. Tangdiongga, T. Koonen, and H. Dorren, "1 × 4 all-optical packet switch at 160 Gb/s employing optical processing of scalable in-band address labels," presented at the Optical Fiber Commun. Conf., San Diego, CA, 2008, Post-Deadline Paper 33.

[19] N. Calabretta, H. D. Jung, E. Tangdiongga, A. M. J. Koonen, and H. J. S. Dorren, "160 Gb/s all-optical packet switching with label rewritings," presented at the Eur. Conf. Opt. Commun., Brussels, Belgium, 2008, Th.3.F.3.

[20] H. J. S Dorren, N. Calabretta, and O. Raz, "A 3-stage CLOS architecture for high-throughput optical packet switching," presented at the Asia Commun. Photonics, Conf. Exhib., Shanghai, China, 2009, FT6.

[21] N. Calabretta, O. Raz, W. Wang, T. Ditewig, F. G. Agis, S. Zhang, H. de Waardt, E. Tangdiongga, and H. J. S. Dorren, "Scalable optical packet switch for optical packets with multiple modulation formats and data rates," presented at the Eur. Conf. Opt. Commun., Vienna, Austria, 2009, We 6.3.4.

[22] E. J. Klein, P. Urban, G. Sengo, L. T. Hilderink, M. Hoekman, R. Pellens, P. van Dijk, and A. Driessen, "Densely integrated microring resonator based photonic devices for use in access networks," *Opt. Express*, vol. 15, no. 16, pp. 10 346–10 355, Aug. 2007.

[23] Y. Liu, E. Tangdiongga, Z. Li, H. de Waardt, A. M. J. Koonen, G. D. Khoe, X. Shu, I. Bennion, and H. J. S. Dorren, "Error-free 320 Gb/s all-optical wavelength conversion using a semiconductor optical amplifier," *J. Lightw. Technol.*, vol. 25, no. 1, pp. 103–108, Jan. 2007.

[24] E. Tangdiongga, Y. Liu, J. H. den Besten, M. van Geemert, T. van Dongen, J. J. M. Binsma, H. de Waardt, G. D. Khoe, M. K. Smit, and H. J. S. Dorren, "Monolithically integrated 80-gb/s AWG-based all-optical wavelength converter," *IEEE Photon. Technol. Lett.*, vol. 18, no. 15, pp. 1627–1629, Aug. 2006.

[25] R. F. Kalman, L. G. Kazovsky, and J. W. Goodman, "Space division switches based on semiconductor optical amplifier," *IEEE Photon. Technol. Lett.*, vol. 4, no. 9, pp. 1048–1051, Sep. 1992.

[26] E. F. Burmeister, J. P. Mack, H. N. Poulsen, J. Klamkin, L. A. Coldren, D. J. Blumenthal, and J. E. Bowers, "SOA gate array recirculating buffer for optical packet switching," presented at the Optical Fiber Commun. Conf., San Diego, CA, 2008, OWe4.

[27] Z. Li, Y. Dong, J. Mo, Y. Wang, and C. Lu, "Cascaded all-optical wavelength conversion for RZ-DPSK signal based on four-wave mixing in semiconductor optical amplifier," *IEEE Photon. Technol. Lett.*, vol. 16, no. 7, pp. 1685–1687, Jul. 2004.

[28] S. Gupta, N. Calabretta, G. Contestabile, E. Ciaramella, and R. Gangopadhyay, "Experimental characterization of SOA based wavelength converters for DPSK signals," in *Proc. ChinaCom*, Beijing, China, 2006, pp. 1–5.

[29] M. Galili, B. Huettl, C. Schmidt-Langhorst, A. Gual i Coca, R. Ludwig, and C. Schubert, "320 Gb/s DQPSK all-optical wavelength conversion using four wave mixing," in *Proc. OFC*, Anaheim, CA, 2007, pp. 25–29.

[30] J. Yu, M.-F. Huang, and G.-K. Chang, "Polarization insensitive wavelength conversion for 4 × 112 Gb/s polarization multiplexing RZ-QPSK signals," *Opt. Express*, vol. 16, no. 26, pp. 21 161–21 169, Dec. 2008.

[31] V. Pusino, P. Minzioni, I. Cristiani, V. Degiorgio, L. Marazzi, P. Boffi, M. Ferrario, P. Martelli, P. Parolari, A. Righetti, R. Siano, M. Martinelli, C. Langrock, and M. M. Fejer, "Wavelength conversion of real-time 100-Gb/s POLMUX RZ-DQPSK," presented at the Optical Fiber Commun. Conf., San Diego, CA, 2009, OThS3.

[32] H. Suche, R. Ludwig, B. Huettl, C. Schmidt-Langhorst, R. Nouroozi, W. Sohler, and C. Schubert, "Polarization insensitive all-optical wavelength conversion of 320 Gb/s RZ-DQPSK data signals," presented at the Optical Fiber Commun. Conf., San Diego, CA, 2009, OThS6.

[33] H. Sun, K.-T. Wu, and K. Roberts, "Real-time measurements of a 40 Gb/s coherent systems," *Opt. Expr.*, vol. 16, no. 2, pp. 873–879, Jan. 2008.